UC Irvine
UC Irvine Previously Published Works

Title
Deficiency in the mouse mitochondrial adenine nucleotide translocator isoform 2 gene is associated with cardiac noncompaction.

Permalink
https://escholarship.org/uc/item/20p2c6x0

Journal
Biochimica et biophysica acta, 1857(8)

ISSN
0006-3002

Authors
Kokoszka, Jason E
Waymire, Katrina G
Flierl, Adrian
et al.

Publication Date
2016-08-01

DOI
10.1016/j.bbabio.2016.03.026

Peer reviewed

eScholarship.org Powered by the California Digital Library
University of California

Biochimica et Biophysica Acta 1857 (2016) 1203–1212

Contents lists available at ScienceDirect

Biochimica et Biophysica Acta

journal homepage: www.elsevier.com/locate/bbabio

Deficiency in the mouse mitochondrial adenine nucleotide translocator isoform 2 gene is associated with cardiac noncompaction☆

Jason E. Kokoszka [a], Katrina G. Waymire [b], Adrian Flierl [c], Katelyn M. Sweeney [d], Alessia Angelin [d], Grant R. MacGregor [b], Douglas C. Wallace [d,*]

[a] Forensic Biology Section, Alabama Department of Forensic Sciences, Annex C, Mobile, AL 36617, United States
[b] Department of Developmental and Cell Biology, University of California Irvine, Irvine, CA 92697-2300, United States
[c] The Parkinson's Institute, Sunnyvale, CA 94085, United States
[d] Center for Mitochondrial and Epigenomic Medicine, Children's Hospital of Philadelphia, Department of Pathology and Laboratory Medicine, University of Pennsylvania, Philadelphia, PA 19104, United States

ARTICLE INFO

Article history:
Received 25 January 2016
Received in revised form 17 March 2016
Accepted 18 March 2016
Available online 24 April 2016

Keywords:
Mitochondria
Heart
Cardiomyopathy
Adenine nucleotide translocator 2 (ANT2)
Hypertrabeculation
Noncompaction

ABSTRACT

The mouse fetal and adult hearts express two adenine nucleotide translocator (ANT) isoform genes. The predominant isoform is the heart–muscle–brain ANT-isoform gene 1 (*Ant1*) while the other is the systemic *Ant2* gene. Genetic inactivation of the *Ant1* gene does not impair fetal development but results in hypertrophic cardiomyopathy in postnatal mice. Using a knockin X-linked *Ant2* allele in which exons 3 and 4 are flanked by *loxP* sites combined in males with a *protamine 1* promoter driven Cre recombinase we created females heterozygous for a null *Ant2* allele. Crossing the heterozygous females with the $Ant2^{fl}$, *PrmCre*(+) males resulted in male and female ANT2-null embryos. These fetuses proved to be embryonic lethal by day E14.5 in association with cardiac developmental failure, immature cardiomyocytes having swollen mitochondria, cardiomyocyte hyperproliferation, and cardiac failure due to hypertrabeculation/noncompaction. ANTs have two main functions, mitochondrial–cytosol ATP/ADP exchange and modulation of the mitochondrial permeability transition pore (mtPTP). Previous studies imply that ANT2 biases the mtPTP toward closed while ANT1 biases the mtPTP toward open. It has been reported that immature cardiomyocytes have a constitutively opened mtPTP, the closure of which signals the maturation of cardiomyocytes. Therefore, we hypothesize that the developmental toxicity of the *Ant2* null mutation may be the result of biasing the cardiomyocyte mtPTP to remain open thus impairing cardiomyocyte maturation and resulting in cardiomyocyte hyperproliferation and failure of trabecular maturation. This article is part of a Special Issue entitled 'EBEC 2016: 19th European Bioenergetics Conference, Riva del Garda, Italy, July 2–6, 2016', edited by Prof. Paolo Bernardi.

© 2016 Elsevier B.V. All rights reserved.

1. Introduction

Mitochondrial dysfunction has frequently been associated with cardiomyopathy. In adults mitochondrial dysfunction can result in hypertrophic or dilated cardiomyopathy [1–3]. In pediatrics, between 0.4 and 5% of live birth infants present with a cardiac malformation. Common among these congenital malformations are ventricular septal defects with cardiac noncompaction being a relatively rare but severe congenital cardiac abnormality [4–6].

Noncompaction of the ventricular myocardium is the persistence of multiple prominent ventricular trabeculations and deep inter-trabecular recesses. Noncompaction is thought to represent an arrest of endomyocardial morphogenesis, which normally occurs between weeks 5 and 8 of human fetal life. Proliferation of the embryonic cardiomyocytes creates the trabecular network which evolves through the gradual compaction of the myocardium, transformation of large intratrabecular spaces into capillaries, and the evolution of the coronary circulation, a process that typically progresses from the epicardium to the endocardium and from the base of the heart to the apex [6].

Mitochondrial dysfunction and disruption of mitochondrial dynamics and the intrinsic pathway for apoptosis have been associated with a variety of cardiac pathologies [1,7]. In a number of cases ventricular noncompaction has been associated with alterations in nuclear DNA (nDNA) coded mitochondrial genes. Barth Syndrome patients and their mouse models can present with noncompaction caused by mutations in the X-linked Tafazzin gene which perturbs mitochondrial cardiolipin metabolism [8,9]. Mice lacking cytochrome c die by E10.5 [10]. Mice with defects in the *Mitofusion 1* & *2* genes or lacking the apoptosis associated genes for caspases 3, 7, 8, FADD and c-FLIP can developed cardiac

☆ This article is part of a Special Issue entitled 'EBEC 2016: 19th European Bioenergetics Conference, Riva del Garda, Italy, July 2–6, 2016', edited by Prof. Paolo Bernardi.

* Corresponding author at: Center for Mitochondrial and Epigenomic Medicine (CMEM), Children's Hospital of Philadelphia, Department of Pathology and Laboratory Medicine, University of Pennsylvania, Colket Translational Research Building, room 6060, 3501 Civic Center Boulevard, Philadelphia, PA 19104, United States.
E-mail address: wallaced1@email.chop.edu (D.C. Wallace).

http://dx.doi.org/10.1016/j.bbabio.2016.03.026
0005-2728/© 2016 Elsevier B.V. All rights reserved.

noncompaction [11–13]. Mice with defects in cardiac Parkin–PINK1-modulated mitophagy can manifest perinatal lethality due to impaired replacement of fetal mitochondria with adult mitochondria [14,15]. Novel mitochondrial DNA (mtDNA) sequence variants have also been reported in noncompaction patients, both in DNAs extracted from patient blood samples [16] and from explanted hearts [17]. Noncompaction hearts have also been found to have a reduced mtDNA copy number in association with mitochondrial ultrastructural abnormalities [17].

To further define the role of mitochondrial dysfunction in cardiomyopathy, we have systemically inactivated the mouse *Ant1* and *Ant2* genes. The ANTs mediate the exchange of ATP and ADP across the mitochondrial inner membrane and thus are central to mitochondrial energy production. They also modulate the mtPTP and thus regulate the intrinsic pathway of apoptosis.

The nature of ANT regulation of both energy metabolism and apoptosis is complex, due to there being multiple ANT isoforms with slightly different properties. Humans have four ANT isoforms [18,19]: ANT1 which is predominantly expressed in the heart and muscle [20–24], ANT2 which is a systemic and inducible [25–27], ANT3 which is also systemic [26], and ANT4 which is testis specific [28]. Mice have three isoforms [29–31]: ANT1 which is expressed in the heart–muscle–brain [30]; ANT2 which is X-linked, expressed in most tissues, and inducible [31]; and ANT4 which is predominantly testis specific [32]. Human ANT1 and ANT3 have been proposed to favor export of ATP from the mitochondrial matrix into the cytosol while ANT2 has been proposed to be kinetically capable of importing cytosolic ATP into the mitochondrial matrix under hypoxic conditions and in cancer cells [33–37].

In addition to the transport of ADP and ATP across the mitochondrial inner membrane, the ANTs have been found to regulate the mtPTP [38]. The mtPTP spans the mitochondrial inner membrane and current data indicates that the mtPTP is composed of components of the ATP synthase, either ATP synthase dimers or the C-ring [39–43]. In differentiated cells, a variety of factors can initiate opening of the mtPTP and apoptosis including reduced mitochondrial inner membrane potential, elevated ADP, elevated reactive oxygen species (ROS), Ca^{++} overload, diamide, and atractyloside, a ligand of the ANTs [2,38].

The different ANT isoforms have different effects on the mtPTP. Over-expression of human ANT1 and ANT3 by transformation of established cell lines with extra *ANT1* and *ANT3* gene copies has been shown to induce apoptosis. However, over-expression of *ANT2* does not have this effect [37,44–47]. The induction of apoptosis by ANT1 does not rely on ATP/ADP transport, but rather is related to amino acids 102–141, the region of greatest divergence between the ANT isoforms [44]. This suggests that the pro-apoptotic action of ANT1 over-expression most likely involves protein–protein interaction. ANT1 but not ANT2 is associated with the IκBα–NFκB complex which is sequestered within the mitochondrion intermembrane space. Over-expression of ANT1 then traps the IκBα–NFκB complexes in the mitochondrion impeding its migration to the nucleus. In the nucleus NFκB transcriptionally activates the *Bcl-XL*, *c-IAP2*, and *Sod2* (MnSOD) genes [46,47]. *Bcl-XL* and *c-IAP2* are anti-apoptotic polypeptides and MnSOD is a mitochondrial matrix enzyme that converts superoxide anion to hydrogen peroxide. Co-expression of cyclophilin D or NFκB with ANT1 inhibits apoptosis confirming that over-expression of ANT1 limits the levels of these anti-apoptotic factors [44,46]. Over-expression of ANT1 must then reduce *Bcl-XL*, *c-IAP2*, and *Sod2* expression favoring the activation (opening) of the mtPTP and increasing matrix ROS production which in differentiated cells would initiate the intrinsic pathway of apoptosis.

Mouse liver mitochondria, which only contain ANT2, still retain a tBHP-sensitive mtPTP when *Ant2* is inactivated. However, the ANT2-deficient mtPTP becomes insensitive to atractyloside and the mtPTP of the ANT2-deficient hepatocytes is intrinsically more sensitive to activation and opening when the cells are treated with increasing concentrations of the calcium ionophore Br-A23187 [38]. These observations suggest that increased ANT1 expression favors the opening of the mtPTP while increased ANT2 expression favors mtPTP closure.

Inactivation of the *Ant1* gene in the mouse has no apparent negative effect on development, with *Ant1* null mice being born at a similar frequency as *Ant1* positive mice. However, by three months of age, the *Ant1* null mice develop a hypertrophic cardiomyopathy [30] which can progress to dilated cardiomyopathy over their two year life span [48]. In humans inactivating mutations in the *ANT1* gene also permit normal development, but results in lifelong cardiomyopathy, the severity of which can be modulated by the individual's mtDNA lineage [49–51]. The systemic inactivation of the mouse *Ant1* gene results in partial inhibition of cardiac mitochondrial ADP-stimulated respiration and increased mitochondrial ROS production. However, the severity of these cardiac effects is not as marked as for the skeletal muscle since in the heart, both ANT1 and ANT2 are expressed while in the muscle ANT1 is the only observed isoform [30,31,52].

Given the cardiac effects of *Ant1* inactivation and the co-expression of ANT1 and ANT2 in the heart, it became important to determine the effect of inactivating the *Ant2* gene on heart function. Surprisingly, unlike *Ant1* null mice, *Ant2* null mice are embryonic lethal. This is associated with a striking cardiac developmental defect including ventricular hypertrabeculation/noncompaction with swollen cardiomyocyte mitochondria, cardiomyocyte hyperproliferation, embryonic lethality by E14.5, and in rare cases neonates with congenital heart defects. Hence, certain types of mitochondrial dysfunction can also contribute to congenital cardiomyopathy.

2. Results

2.1. Differential expression of Ant1 and Ant2 in adult mouse tissues

Mouse somatic tissues differentially express *Ant1* and *Ant2* (Fig. 1). *Ant1* mRNA is present at relatively high levels in the adult skeletal muscle, heart, and to a lesser extent brain and kidney but is absent in the liver. Similarly, ANT1 protein is present at high levels in the heart, skeletal muscle, brain, and to a lesser extent kidney, but is undetectable in the liver. *Ant2* mRNA is present at high levels in the kidney, brain, liver, and heart but is at very low levels in the skeletal muscle, and ANT2 protein is present at high levels in the heart, liver, kidney and brain but is virtually undetectable in the adult skeletal muscle (Fig. 1). Hence, both *Ant1* and *Ant2* are expressed in the adult heart.

2.2. Genetic analysis of Ant2-null mice

To determine the impact of inactivating the *Ant2* gene on cardiac development we employed our mice harboring a conditional knockout allele of the *Ant2* gene [38]. *Ant2* is X-linked [29] and we have substituted the native allele for one in which exons 3 and 4 were flanked by *loxP* sites in the 5′-intron and 3′-untranslated region, creating a functional *Ant2* "floxed" allele (*Ant2*^{fl}, or X^{fl}) [38].

In the current studies, we generated animals lacking ANT2 in all tissues (i.e. a global knockout of the *Ant2* gene) using a *Cre* recombinase transgene transcribed from the *protamine* 1 promoter [53] (X^{fl}Y *PrmCre*(+)). Since the *protamine* promoter is only active during spermiogenesis and genetically haploid sperm share gene products via inter-cellular bridges [54] males hemizygous for both *PrmCre*(+) and the X^{fl} chromosome should transmit a null allele of *Ant2* (X^{del}) in which the last two exons are deleted.

X^{fl}Y, *PrmCre*(+) males were mated with females heterozygous for the X^{fl} and wild type (X^{+}) alleles, resulting in female progeny receiving one deleted allele from the father (X^{del}X^{fl} or X^{del}X^{+}) while the males receive either the X^{fl} or X^{+} from the mothers plus the Y from the fathers. Thus all mice have one active *Ant2* gene. The average litter size of these matings was 10.69 ± 0.73, similar to that seen in crosses in which the male transmitted a functional allele (10.80 ± 1.24, P value = 0.93).

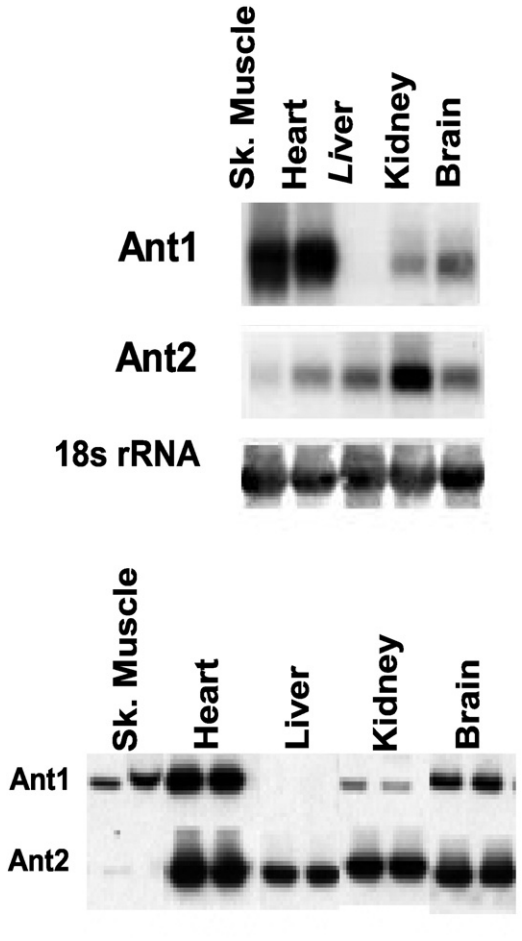

Fig. 1. Differential expression of *Ant1* and *Ant2* in adult tissues. Upper panel: northern blot of the skeletal muscle (Sk. Muscle), heart, liver, kidney, and brain using *Ant1*, *Ant2*, and 18S rRNA riboprobe hybridization. Lower panel: western blot of duplicate samples of the same tissues using isoform specific ANT1 and ANT2 antibodies [30].

Hence, one functional copy of the *Ant2* gene is sufficient for normal development.

When $X^{fl}Y$ *PrmCre*(+) males were crossed with heterozygous ($X^{del}X^{fl}$) *PrmCre*(+) females half of the progeny were global *Ant2* nulls, i.e. either $X^{del}Y$ males or $X^{del}X^{del}$ females, while the remaining pups were $X^{fl}Y$ or $X^{del}X^{fl}$ since the *PrmCre*(+) is not active in females. In these crosses the average litter size was half normal (4.65 ± 0.38) indicating that most of the *Ant2*-deficient mice died embryonically. This is the product of ANT2-deficiency since mice homozygous for the *PrmCre* transgene are viable and fertile. About 5% of the *Ant2*-deficient mice survived to birth, but died as neonates within 16 days.

To determine the stage of embryonic lethality, timed matings were set up between $X^{fl}Y$ *PrmCre*(+) males and $X^{del}X^{fl}$ *PrmCre*(+) females. Equal numbers of control and *Ant2* null embryos were expected, and up to E10.5 the average number of mutant and control embryos in each litter was similar (4.5 ± 0.8 mutants versus 3.3 ± 0.3 controls, n = 6 litters). However, by E12.5 the number of mutant embryos were significantly reduced (2.2 ± 0.1 mutants versus 5.0 ± 0.9 controls, $P < 0.05$, n = 6 litters), and by E14.5 living mutant embryos were rare (0.8 ± 0.5 mutants and 4.3 ± 0.6 controls, $P < 0.01$, n = 4 litters). Beyond E14.5, no viable mutant embryo was recovered in the timed mating experiments (n = 3 litters). Hence, the absence of a functional *Ant2* gene predominantly results in embryonic lethality between embryonic day E10.5 and E14.5.

2.3. Ant2-deficient embryos die of a cardiac defect

To determine the reason for the embryonic lethality of *Ant2*-null mice, control and mutant embryos were recovered from timed matings between E10.5 and E14.5 and anatomically compared. At E10.5, mutant embryos had no overt abnormalities. By E12.5, mutant embryos were slightly smaller than control embryos and appeared pale, consistent with reduced circulation of erythrocytes (Fig. 2). By E14.5 the surviving mutant embryos were clearly runted and lacked erythrocytes in the peripheral vasculature (Fig. 2). Since the cardiac ventricles become fully mature between E12.5 and E14.5, and the most common reason for embryonic loss during this developmental period is cardiac failure [55,56], we hypothesized that the primary defect in the *Ant2*-mutant embryos was due to cardiac dysfunction.

To test this hypothesis, embryos from timed matings were recovered, fixed or frozen, and cardiac development examined histologically. At E10.5, mutant embryos appeared similar to controls. By E14.5 the mutant embryos exhibited striking cardiac abnormalities including malformed or absent interventricular septum, hypoplastic ventricle walls, dilated atria (Fig. 3, Panel A), and pronounced and persistent trabeculae (Fig. 3, Panel B). No other tissues showed gross pathological changes, though some tissues appeared underdeveloped.

Ultrastructural examination of the ventricular walls of the control and mutant mice revealed that many of the muscle fibers of the mutant E14.5 embryos were disrupted and surviving myocardial cells contained large numbers of cytosolic electron-dense particles (Fig. 4, Panel A). The ANT2-deficient cardiomyocyte mitochondria were swollen with twice the area of control cardiomyocyte mitochondria (ANT2-deficient mitochondrial area was 2.34 ± 1.39 μm^2, mean ± SD, n = 196 mitochondria, n = 16 cardiomyocytes, n = 4 mice; ANT2-positive mitochondrial area 1.05 ± 0.65 μm^2, n = 126 mitochondria, n = 11 cardiomyocytes, n = 2 mice). The mitochondria of the ANT2-deficient cardiomyocytes also had reduced cristae and in some cases intra-mitochondrial inclusions (Fig. 4, Panel B).

Mitochondrial abnormalities were even more pronounced in the cardiomyocytes of the few ANT2-deficient animals that survived to term. At postnatal day (P) 13 the mitochondria were dramatically enlarged, cristae density was severely diminished, and clear areas (lucencies) within the matrix were common (Fig. 4, Panel C).

2.4. Ant1 and Ant2 expression in the embryonic heart

One possible reason for the striking difference in embryonic development between ANT1- and ANT2-null mice could be that only *Ant2* is expressed in the embryonic heart. However, when mRNA levels were analyzed by in situ hybridization and real time PCR, both *Ant1* and *Ant2* mRNAs were expressed in the heart (Fig. 5). Using isoform-specific riboprobes for *Ant1* and *Ant2*, paraffin embedded embryonic *Ant1* and *Ant2* positive heart sections were analyzed for differential gene expression by in situ hybridization. Cardiac sections from *Ant1* or *Ant2* null embryos were used as negative controls. With this analysis both *Ant1* and *Ant2* mRNAs were detected in the hearts of E10.5, E12.5, and E14.5 mouse embryos (Fig. 5, Panel A).

The relative levels of the *Ant1* and *Ant2* mRNAs were then quantified by real time PCR. *Ant1* mRNA was found to be about five times the level of *Ant2* in 8 pooled E14.5 control embryonic hearts (3.96 ± 1.12 fg/μl versus 0.69 ± 0.11 fg/μl, respectively) (Fig. 5, Panel B). Additional evidence that *Ant1* is expressed in the embryonic heart was obtained using our transgenic mouse in which the *β-Geo* promoter-less exon containing the β-galactosidase open reading frame was fused in frame to the second exon of the *Ant1* gene. In these mice, the *Ant1-βGeo* fusion mRNA is transcribed from the endogenous *Ant1* promoter and the mRNA translated using Ant1 mRNA translation signals [30]. Staining E11.5 *Ant1-βGeo* heterozygous mice with X-gal revealed very strong β-galactosidase activity in the heart (Fig. 5, Panel C). Therefore, the *Ant1* gene is transcribed in the embryonic heart and the mRNA translated

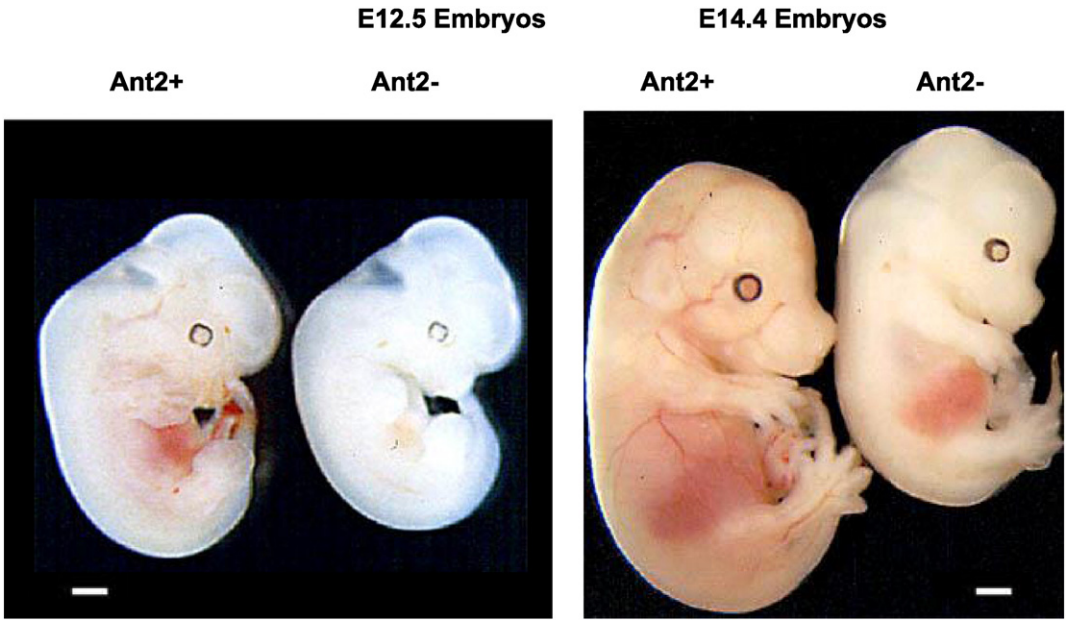

Fig. 2. Phenotype of E12.5 and E14.5 control and *Ant2*-null embryos. Control littermate embryos are on the left and *Ant2*-deficient embryos are on the right. E12.5 embryos show grossly normal development but are smaller. Scale bar = 1 mm. E14.5 embryos showing more dramatic runting. Scale bar = 1 mm.

into functional protein. Hence, the pronounced cardiac developmental defect in the *Ant2*-mutant mice is not due to its being the only embryonic cardiac ANT. Rather the cardiac developmental defect must be the result of loss of a unique ANT2 function that cannot be compensated by ANT1.

2.5. Cardiomyocyte proliferation in the embryonic heart

To determine if the *Ant2*-deficiency caused the cardiac defect by limiting cardiomyocyte proliferation or increased cardiomyocyte cell death, embryonic cardiomyocyte DNA synthesis was analyzed using 5′-bromo-deoxyuridine (BrdU) incorporation. Pregnant females were injected with BrdU at E14.5, sacrificed 2 h later, and the embryos quantified for the incorporation of the BrdU into actively replicating cardiomyocyte nuclei. Nuclei that incorporated BrdU into their DNA were detected using an anti-BrdU antibody, and all nuclei were identified by counterstaining with Hoechst 33342 (Fig. 6, Panel A). Surprisingly, the ratio of replicating nuclei to total cardiomyocyte nuclei was significantly higher in the *Ant2*-mutant embryos than in control embryos in the ventricle wall (VW), interventricular septum (IVS), and trabeculae (Trab.) (Fig. 6, Panel B).

To determine if ANT2-deficiency resulted in increased cardiomyocyte apoptosis in the developing heart, TUNEL analysis was performed. However, no significant differences were observed in cardiomyocytes at E13.5 or E14.4. Thus, the cardiac developmental abnormalities of the *Ant2*-mutant embryos are not due to inhibition of cardiomyocyte proliferation or to increased apoptosis rates.

3. Discussion

To investigate the role of mitochondrial dysfunction in cardiomyopathy, we have systemically inactivated the mouse *Ant1* and *Ant2* genes. Inactivation of *Ant1* permits normal fetal development and results in animals that manifest hypertrophic cardiomyopathy which can progress to dilated cardiomyopathy [30,48]. Inactivation of *Ant2* results in sever cardiac developmental defects including hypoplasia of the ventricular walls, ventricular septal defects, hyperproliferation of disorganized cardiomyocytes, swollen mitochondria with minimal internal cristae structure, and noncompaction of the trabecular network. *Ant2*-mutation disruption of cardiomyocyte function results in embryonic lethality by E14.5 in the great majority of cases, though a small percentage of *Ant2* null mice are born and manifest congenital heart defects with swollen mitochondria.

The differences in ANT1- versus ANT2-null phenotypes are not due to ANT2 being the sole ANT expressed during cardiac development since ANT1 is expressed at much higher levels in the developing heart than ANT2. Since ANT1 is more adept at mitochondrial ATP export than ANT2, it also seems unlikely that the cause of the *Ant2*-null developmental defect is deficiency in ATP levels. Finally, the hyperproliferation of the cardiomyocytes and the lack of increased apoptosis indicates that the abnormal cardiac development is not due to a deficiency in the number of cardiomyocytes.

An alternative hypothesis is that *Ant1* and *Ant2* inactivation could have differential effects on the modulation of the mtPTP. The timing of the cardiac pathology associated with ANT2-deficiency coincides with the transition of mouse immature cardiomyocytes into mature cardiomyocytes between E9.5 and E13.5. In wild type mice, immature cardiomyocytes have swollen mitochondria with minimal internal structure as well as reduced mitochondrial membrane potential, constitutively open mtPTPs, and high mitochondrial ROS production. The maintenance of an open mtPTP and high ROS production keeps the embryonic cardiomyocytes in the immature state [57].

Between embryonic day E9.5 and E13.5, mouse immature cardiomyocytes progress to mature cardiomyocytes. As the cardiomyocytes mature toward E13.5 the mitochondria become elongated, the mitochondrial membrane potential increases along with ATP production, mitochondrial ROS production declines, and the mtPTP closes. The ANTs directly regulate this cardiomyocyte maturation since immature mouse cardiomyocytes treated with the ANT agonist carboxyatractyloside which keeps the mtPTP open are inhibited in cardiomyocyte maturation while treatment of immature cardiomyocytes with the ANT antagonist bongkrekic acid closes the mtPTP and results in enhanced cardiomyocyte maturation [57,58].

Since the ANT ligands carboxyatractyloside and bongkrekic acid differentially modulate the mtPTP and the maturation of the E9.5 cardiomyocytes, it follows that the genetic manipulation of the *Ant1* and *Ant2* genes might also modulate the mtPTP and perturb cardiomyocyte maturation. Transformation of cancer cells with extra copies of ANT1 induce apoptosis [37,44–46], the pro-apoptotic potential of increased ANT1 being linked to its ability to sequester IκBα–NFκB complexes and thus inhibit the expression of the anti-apoptotic genes

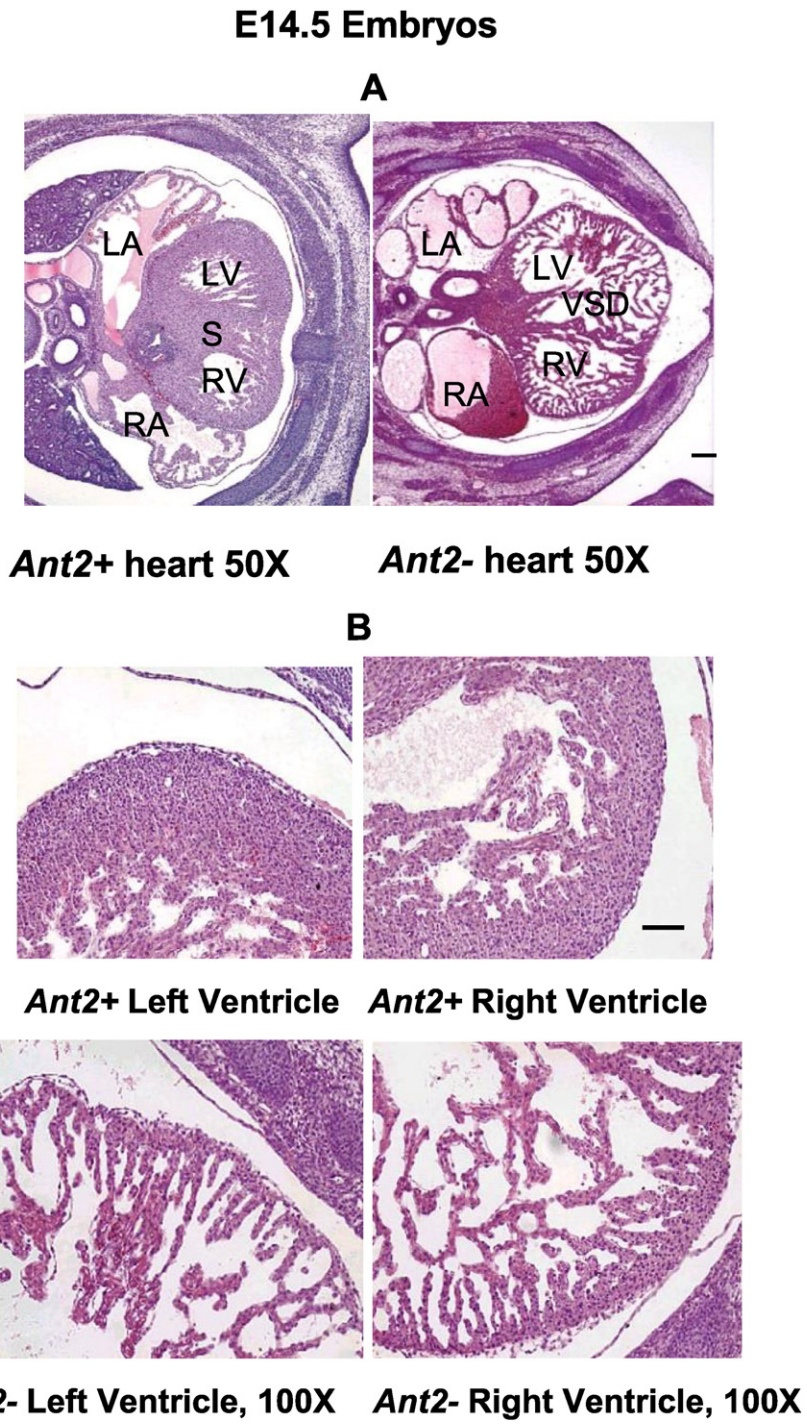

Fig. 3. E14.5 *Ant2*− versus *Ant2*+ embryos exhibit septal defects, reduced compaction zone, and abnormal trabeculae. Hematoxylin and eosin stained cardiac sections. Panel A: 50× photomicrographs of transverse sections of *Ant2*+ (left) and *Ant2*− (right) embryos showing marked septal defects, ventricular wall hypoplasia, persistent trabeculation and noncompaction of the *Ant2*− heart. LA = left atrium; RA = right atrium; LV = left ventricle; RV = right ventricle; S = septum; VSD = ventricular septal defect. Scale bar = 200 μm; Panel B: Left and right ventricles showing persistence of trabecular network, hypoplasia of the ventricular walls and noncompaction in the ANT2-deficient hearts (bottom) versus controls (top). Scale Bar = 50 μm.

Bcl-XL, *c-IAP2*, and *Sod2* [46]. Since the intrinsic pathway of apoptosis is coupled with the activation and opening of the mtPTP, over expression of ANT1 must bias the mtPTP to be open. This may explain why ANT1 is expressed at such high levels in early cardiac development, a time when it is important for the mtPTP to be open. Conversely, knockout of *Ant1* would increase NFκB signaling, elevating the expression of the anti-apoptotic Bcl-XL and c-IAP2 polypeptides plus MnSOD. This would bias the cardiomyocyte mtPTP to close thus favoring cardiomyocyte maturation and normal heart development, thus explaining why ANT1-deficiency is consistent with a normal progression in cardiac development.

Conversely, in proliferating cells including cancer cells ANT2 is up-regulated, and its knockdown in cancer cells promotes apoptosis [59–61]. Since cancer cells must inhibit apoptosis to survive and

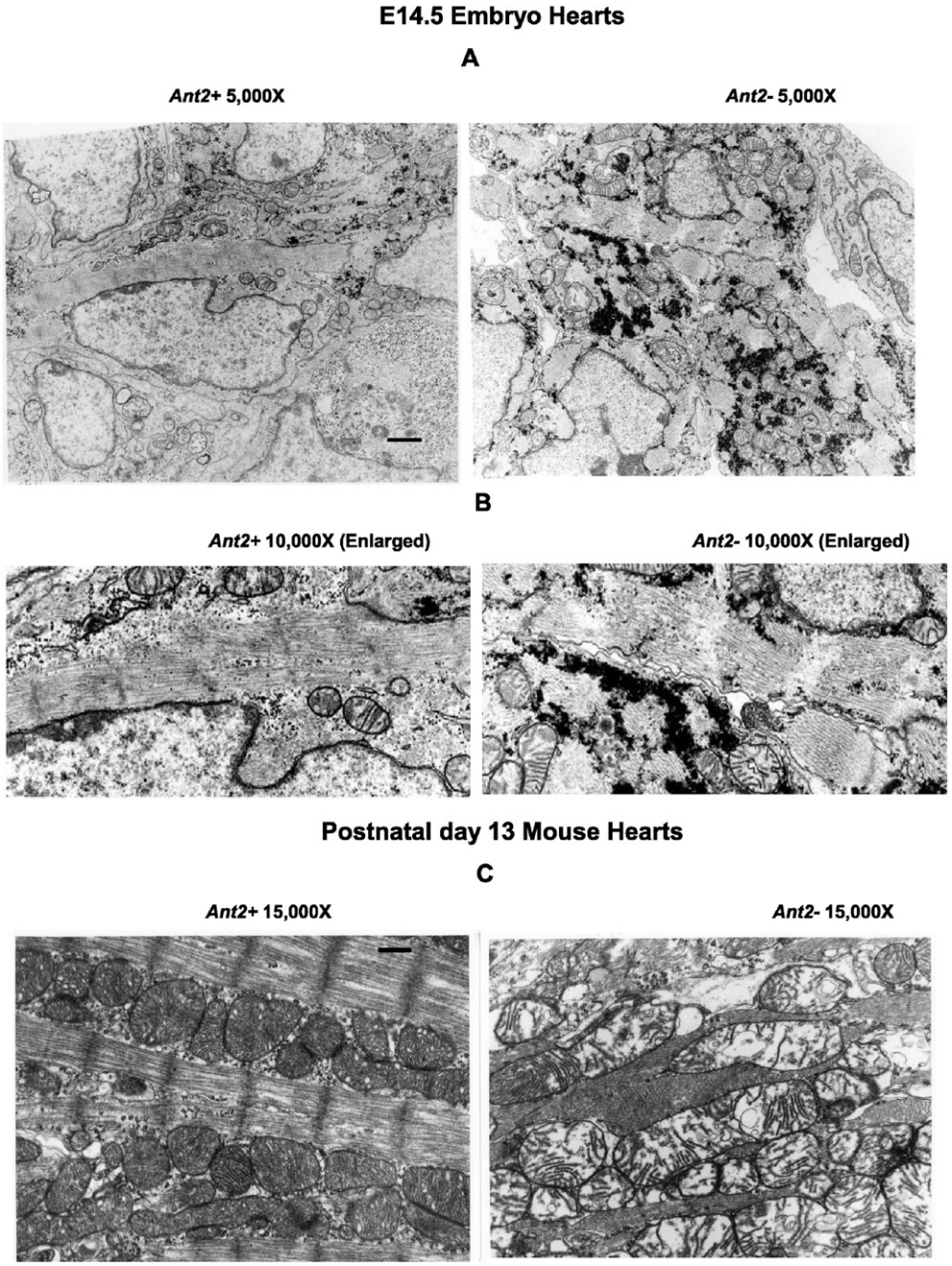

Fig. 4. Ultra-structure of cardiac ventricular wall in *Ant2*− versus *Ant2*+ mice. Panel A: E14.5 *Ant2*+ left and *Ant2*− right cardiomyocyte electron micrographs (5000×) showing that *Ant2*− cardiomyocytes have disorganized contractile fibers, swollen and enlarged mitochondria with few cristae, and frequent matrix lucencies. Scale bar = 2 μm. Panel B: E14.5 *Ant2*+ left and *Ant2*− right electron micrographs (10,000×) of cardiomyocytes showing that *Ant2*− cardiomyocytes have disrupted contractile elements and accumulation of electron dense precipitates within the cytoplasm. Panel C: Electron micrographs (15,000×) of ventricular cardiomyocytes from post-natal day (P) 13 *Ant2*+ left and *Ant2*− right mice showing swollen and enlarged mitochondria with few cristae, and frequent matrix lucencies in *Ant2*− animal. Scale bar = 0.5 μm.

activation of the mtPTP to open promotes apoptosis, it follows that up-regulation of ANT2 must stabilize the mtPTP in the closed configuration thus inhibiting apoptosis.

ANT2-null hepatocytes are more prone to mtPTP opening and apoptosis when exposed to Br-A23187 [38] and the mitochondria of both ANT2-null embryonic and 13 day old mouse cardiomyocytes have swollen mitochondria with few cristae and more internal lucencies, morphological features characteristic of mitochondria having an activated and thus open mtPTP. Therefore, it would seem likely that ANT2-deficiency in cardiomyocytes favors an open mtPTP. This would bias the cardiomyocytes to remain in the immature state which would explain why the ANT2-null cardiomyocytes have fewer and less organized contractile fibers [57]. Finally, inhibition of cardiomyocyte maturation would permit continued proliferation of the immature cardiomyocytes ultimately resulting in cardiac trabeculation/noncompaction and embryonic lethality.

In conclusion, genetic inactivation of ANT1 permits cardiac development but predisposes the adult to hypertrophic and dilated cardiomyopathy, presumably due to impaired mitochondrial ATP production. By contrast, genetic inactivation of ANT2 results in impaired cardiac development, possibly due to altered regulation of the mtPTP which inhibits embryonic cardiomyocyte maturation. Hence, mitochondrial dysfunction can be an important contributor to the etiology of either adult of pediatric cardiomyopathy, depending on which of the multifaceted functions of the mitochondria are perturbed.

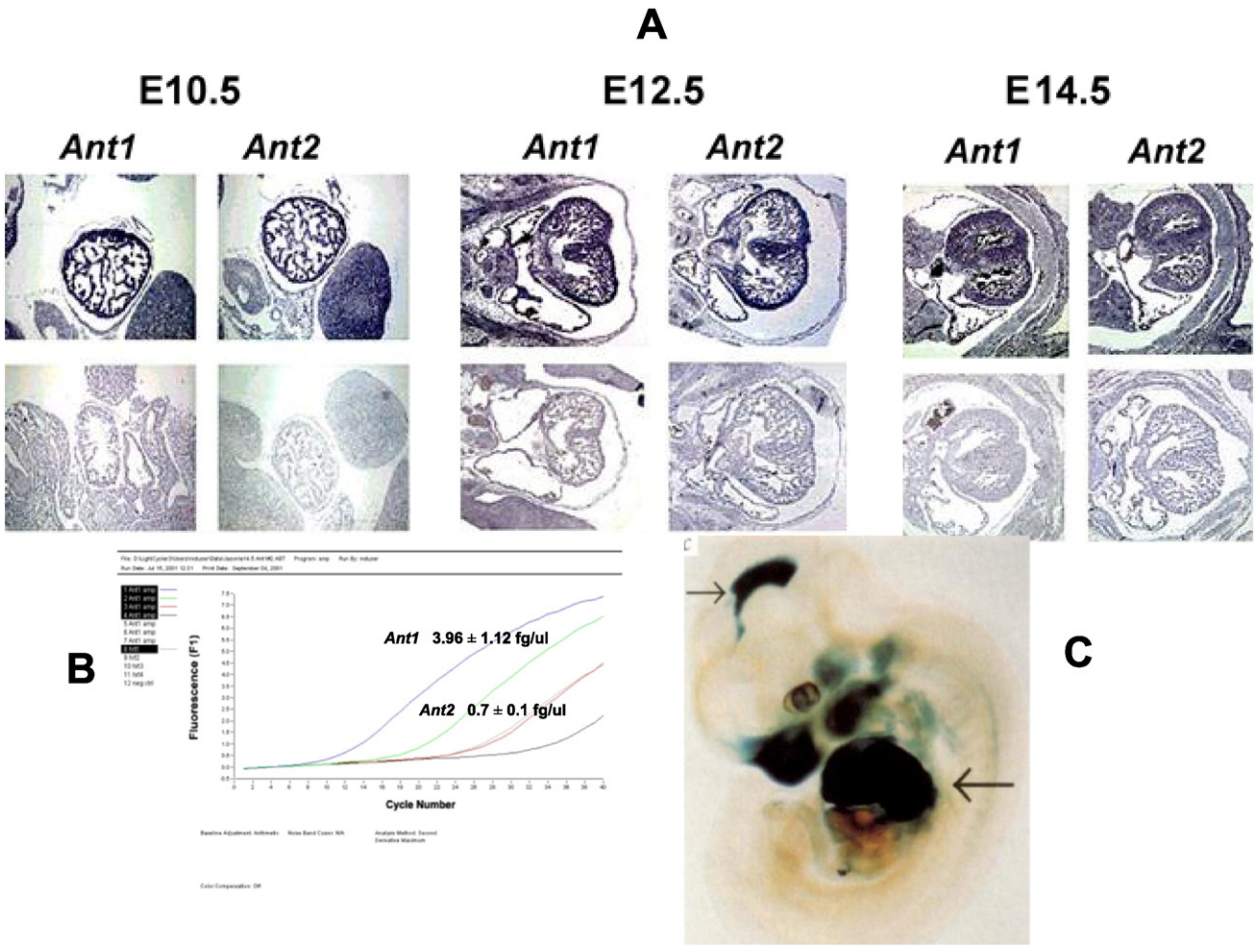

Fig. 5. Expression of *Ant1* and *Ant2* in the embryonic heart. Panel A: In situ hybridization was performed using E10.5, E12.5, and E14.5 embryo sections. The top row contains sections of control (*Ant1* + & *Ant2* +) hybridized with *Ant1* and *Ant2* riboprobes. Both riboprobes hybridize strongly to the embryonic heart of *Ant1* + & *Ant2* + mice throughout cardiac development. The bottom row of sections are negative controls derived from alternating *Ant1* − & *Ant2* + and *Ant1* + & *Ant2* − hearts hybridized to the riboprobe of the deleted mouse gene. The lack of cross hybridization confirms the specificity of the riboprobes. Panel B: Quantitative Real Time PCR of *Ant1* and *Ant2* mRNAs in E14.5 hearts. Blue and Green lines are repeats of *Ant1* mRNA amplification kinetics while the red and light gray lines are repeats of *Ant2* mRNA amplification. The dark gray line is the amplification of a housekeeping control gene. The higher average amplification rate indicates that there is on average 5× more *Ant1* than *Ant2* mRNA. Panel C: Proof that ANT1 protein is expressed in the fetal heart is demonstrated by the expression of the *Ant1-βGeo* knockin gene containing the β-galactosidase open reading frame fused in-frame with the second exon of *Ant1*. With this construct the E11.5 heart stains strongly blue with X-gal confirming Ant1 protein expression.
Figure reproduced from [30].

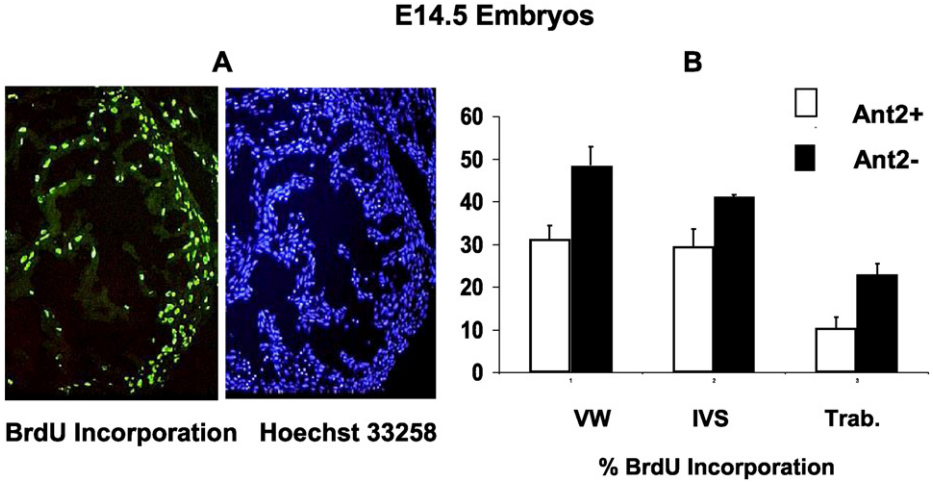

Fig. 6. Cardiomyocyte proliferation in E14.5 embryo *Ant2* + and *Ant2* − mice. Panel A, left: Representative image of fetal heart BrdU incorporation, with cells having replicated and incorporated BrdU being identified by immunohistochemistry using anti-BrdU incorporated DNA antibody. Panel A, right: Representative image of total cardiomyocyte nuclei number detected by Hoechst 33342 staining and fluorescence. Panel B: The proportion of replicating cardiomyocyte nuclei in *Ant1* + & *Ant2* + control embryonic hears (□, n = 3) and *Ant1* + & *Ant2* − mutant hearts ((■, n = 3) showing elevated cardiomyocyte replication within the ventricular wall (VW) ($P < 0.05$), interventricular septum (IVS) ($P < 0.05$), and trabecular network (Trab.) ($P < 0.05$) in the *Ant2* − hearts.

4. Materials and methods

4.1. Mouse genetics

All mice were on a hybrid background, fed Purina Labdiet 5021, and housed at 20 °C with a 13 h on, 11 h off light cycle. For biochemical analyses, animals were euthanized by cervical dislocation. All animal procedures were performed in accordance with Emory University's ethical guidelines outlined in an Institutional Animal Care and Use Committee approved protocol.

A targeting vector with exons 3 and 4 flanked by *loxP* sites and containing a *PGK-neo* cassette was electroporated into the male ES cell line AK7.1. Properly targeted cells were selected in G418 and confirmed by Southern blot using multiple probes. The 5′-probe detects a 6604 bp *Xba I* fragment for the targeted locus and a 12,828 bp fragment for the wild type locus. The recombinant allele gave a 9380 bp *Xba I* fragment detected with the 5′-probe. The 3′-probe detects a 13,781 bp *Dra III* fragment for the targeted locus and a 7961 bp fragment for the wild type.

Site-specific recombination between the *loxP* sites removed the last 1/3 of the ANT2 protein and the *PGK-neo* cassette. The deleted region included the putative transmembrane domains 5 and 6 and generated a non-functional protein.

Ant2 global knockout embryos were genotyped by extracting DNA from yolk sacs, and *Ant1*$^{-/-}$ postnatal mice were genotyped using toe DNA as template. The *Ant1* and *Ant2* loci were genotyped by PCR amplification, *Ant1* as described [30] and *Ant2* locus using the forward primer 5′ ACTCAACCTAGGGCCTTGTG 3′ and the reverse primer 5′ GGGAGCAT TCCTGAAAAATAA 3′ (35 cycles of PCR: 94 °C for 20 s, 56 °C for 30 s, and 72 °C for 40 s) to detect the *loxP* insertion. The targeted *Ant2* locus generated a 485 bp product while the wild type locus gave a 354 bp product. The recombinant *Ant2* allele was detected with the same forward primer and the reverse primer 5′ GACTTACCCTCCACGACAGC 3′. With the PCR conditions used (35 cycles, 94 °C for 20 s, 65 °C for 30 s, and 72 °C for 60 s), an 850 bp product was amplified when the recombination event occurred, the unrecombined allele (4.0 kb) being too large to amplify. All PCR products were initially sequence verified to ensure the fidelity of the genotyping protocols. These methods have been previously summarized [38].

4.2. Histological analysis

Embryos were dissected out of pregnant females and fixed in 4% paraformaldehyde overnight and dehydrated in increasing concentrations of ethanol and then embedded in paraffin. Specimens were sectioned at 6 μm and stained with hematoxylin and eosin. For electron microscopy, samples were dissected, and placed in 4% glutaraldehyde fixative for 4 h at room temperature. Samples were then processed for staining, embedding, sectioning, and post-staining. Specimens were examined and photographed with a Philips CM-10 electron microscope.

4.3. Ant expression

For in situ hybridization analysis embryos were fixed overnight in 2% paraformaldehyde and washed in PBS. Embryos were then dehydrated in increasing concentrations of ethanol and embedded in paraffin and sectioned at 6 μm. Digoxygenin (DIG)-labeled riboprobes [62] specific for *Ant1* and *2* were generated from the 3′UTR and exon 4. The riboprobes encompassed cDNA nucleotides 817 to 1093 for *Ant1* and 834 to 1244 for *Ant2* [63]. Sections were deparaffinized, rehydrated, acetylated, and dehydrated. Specimens were then pre-hybridized for 1 h and hybridized with riboprobe overnight. Samples were washed, blocked with sheep serum, incubated with the anti-DIG antibody overnight, and then incubated with nitroblue tetrazolium to visualize riboprobe hybridization.

Real-time quantitative PCR was performed to determine the amounts of *Ant1* and *Ant2* mRNAs present in embryonic hearts. Eight–ten wild type E14.5 mouse hearts were pooled together, RNA isolated, and cDNA synthesized (Gibco-BRL, USA). Aliquots of the cDNA were used as template for real-time PCR with primers specific for *Ant1* (forward primer 5′ GACCCCAAGAATGTGCACAT 3′ and the reverse primer 5′ TTGTGAGC TTGGGTATTACAC 3′) and *Ant2* (forward primer 5′ AGCTGGATGATTGC ACAGTC 3′ and the reverse primer 5′ ACAGACAAGCCCAGAGAATC 3′). A standard curve consisting of known amounts of *Ant1* or *Ant2* cDNA was performed with each analysis (n = 3).

4.4. Western blot analysis

Isoform-specific ANT1 and ANT2 antibodies [30] were reacted, using Western Blot Kits (Kirkegaard & Perry Laboratories) to isolated mitochondrial protein (20 μg) or supernatants separated by SDS-PAGE and blotted onto nitrocellulose.

4.5. Cardiomyocyte proliferation analyses

To assess cardiomyocyte proliferation, pregnant females were injected with 50 mg of BrdU/kg body weight 2 h before sacrificing. The embryos were fixed overnight in 2% paraformaldehyde, processed in sequential sucrose concentrations of 10, 15, and 20%, incubated overnight at 4 °C in a solution of 1 part cryo-OCT and 1 part 20% sucrose, and embedded in a solution of 3 parts cryo-OCT and 1 part 20% sucrose. Specimens were cryo-sectioned at 6 μm, depurinated, neutralized, permeabilized, and incubated with goat anti-BrdU antibody (Harlan Sera-Lab, Leicestershire, England). A sheep anti-goat antibody (Jackson Labs, West Grove, PA, USA) conjugated with fluorescein was used to detect BrdU-incorporation. Sections were counterstained using 5 μM Hoechst 33342. Fluorescein and Hoechst fluorescence were detected using a Zeiss-Axiophot™ microscope equipped with fluorescent optics. Three control and three mutant embryos were analyzed with approximately 500 heart nuclei counted per embryo.

Apoptotic cardiomyocytes were counted in 10-micron thick isopentane frozen cardiac sections by TUNEL staining using the In Situ Cell Death Detection Kit (Roche Molecular Biochemicals, Indianapolis, IN). Three control and three mutant embryos were analyzed with approximately 500 heart nuclei examined per embryo.

4.6. Statistical analysis

Data analysis was carried out with GRAPHPAD PRISM software (GraphPad, San Diego). P values represent the results of the Student's unpaired *t* test.

Transparency document

The transparency document associated with this article can be found, in online version.

Acknowledgements

We would like to acknowledge Dr. Stephen O'Gorman for providing the *PrmCre* transgenic mice. This work was supported by NIH grants NS021328, CA182384, and NS41850 awarded to DCW.

References

[1] G.A. Porter Jr., J. Hom, D. Hoffman, R. Quintanilla, K. de Mesy Bentley, S.S. Sheu, Bioenergetics, mitochondria, and cardiac myocyte differentiation, Prog. Pediatr. Cardiol. 31 (2011) 75–81.

[2] D.C. Wallace, M.T. Lott, V. Procaccio, Mitochondrial medicine: the mitochondrial biology and genetics of metabolic and degenerative diseases, cancer, and aging, in: D.L. Rimoin, R.E. Pyeritz, B.R. Korf (Eds.), Emery and Rimoin's Principles and Practice of Medical Genetics, Churchill Livingstone Elsevier, 2013.

[3] E. Murphy, H. Ardehali, R.S. Balaban, F. DiLisa, G.W. Dorn II, R.N. Kitsis, K. Otsu, P. Ping, R. Rizzuto, M.N. Sack, D.C. Wallace, R.J. Youle, AHA position paper on mitochondrial function, biology and role in disease, J. Am. Heart Assoc. (2016) (in press).
[4] J.I. Hoffman, S. Kaplan, The incidence of congenital heart disease, J. Am. Coll. Cardiol. 39 (2002) 1890–1900.
[5] M.E. Pierpont, C.T. Basson, D.W. Benson Jr., B.D. Gelb, T.M. Giglia, E. Goldmuntz, G. McGee, C.A. Sable, D. Srivastava, C.L. Webb, Genetic basis for congenital heart defects: current knowledge: a scientific statement from the American Heart Association Congenital Cardiac Defects Committee, Council on Cardiovascular Disease in the Young: endorsed by the American Academy of Pediatrics, Circulation 115 (2007) 3015–3038.
[6] R.H. Pignatelli, C.J. McMahon, W.J. Dreyer, S.W. Denfield, J. Price, J.W. Belmont, W.J. Craigen, J. Wu, H. El Said, L.I. Bezold, S. Clunie, S. Fernbach, N.E. Bowles, J.A. Towbin, Clinical characterization of left ventricular noncompaction in children: a relatively common form of cardiomyopathy, Circulation 108 (2003) 2672–2678.
[7] M.V. Zaragoza, M.C. Brandon, M. Diegoli, E. Arbustini, D.C. Wallace, Mitochondrial cardiomyopathies: how to identify candidate pathogenic mutations by mitochondrial DNA sequencing, MITOMASTER and phylogeny, Eur. J. Hum. Genet. 19 (2011) 200–207.
[8] B. Chang, N. Momoi, L. Shan, M. Mitomo, Y. Aoyagi, K. Endo, I. Takeda, R. Chen, Y. Xing, X. Yu, S. Watanabe, T. Yoshida, H. Kanegane, S. Tsubata, N.E. Bowles, F. Ichida, T. Miyawaki, Gonadal mosaicism of a TAZ (G4.5) mutation in a Japanese family with Barth syndrome and left ventricular noncompaction, Mol. Genet. Metab. 100 (2010) 198–203.
[9] C.K. Phoon, D. Acehan, M. Schlame, D.L. Stokes, I. Edelman-Novemsky, D. Yu, Y. Xu, N. Viswanathan, M. Ren, Tafazzin knockdown in mice leads to a developmental cardiomyopathy with early diastolic dysfunction preceding myocardial noncompaction, J. Am. Heart Assoc. 1 (2012) (jah3-e000455).
[10] K. Li, Y. Li, J.M. Shelton, J.A. Richardson, E. Spencer, Z.J. Chen, X. Wang, R.S. Williams, Cytochrome c deficiency causes embryonic lethality and attenuates stress-induced apoptosis, Cell 101 (2000) 389–399.
[11] A. Kasahara, S. Cipolat, Y. Chen, G.W. Dorn II, L. Scorrano, Mitochondrial fusion directs cardiomyocyte differentiation via calcineurin and Notch signaling, Science 342 (2013) 734–737.
[12] S.A. Lakhani, A. Masud, K. Kuida, G.A. Porter Jr., C.J. Booth, W.Z. Mehal, I. Inayat, R.A. Flavell, Caspases 3 and 7: key mediators of mitochondrial events of apoptosis, Science 311 (2006) 847–851.
[13] W.C. Yeh, A. Itie, A.J. Elia, M. Ng, H.B. Shu, A. Wakeham, C. Mirtsos, N. Suzuki, M. Bonnard, D.V. Goeddel, T.W. Mak, Requirement for Casper (c-FLIP) in regulation of death receptor-induced apoptosis and embryonic development, Immunity 12 (2000) 633–642.
[14] G. Gong, M. Song, G. Csordas, D.P. Kelly, S.J. Matkovich, G.W. Dorn II, Parkin-mediated mitophagy directs perinatal cardiac metabolic maturation in mice, Science 350 (2015) aad2459.
[15] Y. Kageyama, M. Hoshijima, K. Seo, D. Bedja, P. Sysa-Shah, S.A. Andrabi, W. Chen, A. Hoke, V.L. Dawson, T.M. Dawson, K. Gabrielson, D.A. Kass, M. Iijima, H. Sesaki, Parkin-independent mitophagy requires Drp1 and maintains the integrity of mammalian heart and brain, EMBO J. 33 (2014) 2798–2813.
[16] S. Tang, A. Batra, Y. Zhang, E.S. Ebenroth, T. Huang, Left ventricular noncompaction is associated with mutations in the mitochondrial genome, Mitochondrion 10 (2010) 350–357.
[17] S. Liu, Y. Bai, J. Huang, H. Zhao, X. Zhang, S. Hu, Y. Wei, Do mitochondria contribute to left ventricular non-compaction cardiomyopathy? New findings from myocardium of patients with left ventricular non-compaction cardiomyopathy, Mol. Genet. Metab. 109 (2013) 100–106.
[18] G. Stepien, A. Torroni, A.B. Chung, J.A. Hodge, D.C. Wallace, Differential expression of adenine nucleotide translocator isoforms in mammalian tissues and during muscle cell differentiation, J. Biol. Chem. 267 (1992) 14592–14597.
[19] P.Y. Dupont, A. Guttin, J.P. Issartel, G. Stepien, Computational identification of transcriptionally co-regulated genes, validation with the four ANT isoform genes, BMC Genomics 13 (2012) 482.
[20] N. Neckelmann, K. Li, R.P. Wade, R. Shuster, D.C. Wallace, cDNA sequence of a human skeletal muscle ADP/ATP translocator: lack of a leader peptide, divergence from a fibroblast translocator cDNA, and coevolution with mitochondrial DNA genes, Proc. Natl. Acad. Sci. U. S. A. 84 (1987) 7580–7584.
[21] A.B. Chung, G. Stepien, Y. Haraguchi, K. Li, D.C. Wallace, Transcriptional control of nuclear genes for the mitochondrial muscle ADP/ATP translocator and the ATP synthase beta subunit. Multiple factors interact with the OXBOX/REBOX promoter sequences, J. Biol. Chem. 267 (1992) 21154–21161.
[22] Y. Haraguchi, A.B. Chung, A. Torroni, G. Stepien, J.M. Shoffner, J.J. Wasmuth, D.A. Costigan, M. Polak, M.R. Altherr, S.T. Winokur, D.C. Wallace, Genetic mapping of human heart–skeletal muscle adenine nucleotide translocator and its relationship to the facioscapulohumeral muscular dystrophy locus, Genomics 16 (1993) 479–485.
[23] K. Li, J.A. Hodge, D.C. Wallace, OXBOX, a positive transcriptional element of the heart–skeletal muscle ADP/ATP translocator gene, J. Biol. Chem. 265 (1990) 20585–20588.
[24] K. Li, C.K. Warner, J.A. Hodge, S. Minoshima, J. Kudoh, R. Fukuyama, M. Maekawa, Y. Shimizu, N. Shimizu, D.C. Wallace, A human muscle adenine nucleotide translocator gene has four exons, is located on chromosome 4, and is differentially expressed, J. Biol. Chem. 264 (1989) 13998–14004.
[25] R. Battini, S. Ferrari, L. Kaczmarek, B. Calabretta, S.T. Chen, R. Baserga, Molecular cloning of a cDNA for a human ADP/ATP carrier which is growth-regulated, J. Biol. Chem. 262 (1987) 4355–4359.
[26] J. Houldsworth, G. Attardi, Two distinct genes for ADP/ATP translocase are expressed at the mRNA level in adult human liver, Proc. Natl. Acad. Sci. U. S. A. 85 (1988) 377–381.
[27] A.L. Cozens, M.J. Runswick, J.E. Walker, DNA sequences of two expressed nuclear genes for human mitochondrial ADP/ATP translocase, J. Mol. Biol. 206 (1989) 261–280.
[28] V. Dolce, P. Scarcia, D. Iacopetta, F. Palmieri, A fourth ADP/ATP carrier isoform in man: identification, bacterial expression, functional characterization and tissue distribution, FEBS Lett. 579 (2005) 633–637.
[29] J.W. Ellison, E.C. Salido, L.J. Shapiro, Genetic mapping of the adenine nucleotide translocase-2 gene (Ant2) to the mouse proximal X chromosome, Genomics 36 (1996) 369–371.
[30] B.H. Graham, K.G. Waymire, B. Cottrell, I.A. Trounce, G.R. MacGregor, D.C. Wallace, A mouse model for mitochondrial myopathy and cardiomyopathy resulting from a deficiency in the heart/skeletal muscle isoform of the adenine nucleotide translocator, Nat. Genet. 16 (1997) 226–234.
[31] S.E. Levy, Y. Chen, B.H. Graham, D.C. Wallace, Expression and sequence analysis of the mouse adenine nucleotide translocase 1 and 2 genes, Gene 254 (2000) 57–66.
[32] N. Rodic, M. Oka, T. Hamazaki, M.R. Murawski, M. Jorgensen, D.M. Maatouk, J.L. Resnick, E. Li, N. Terada, DNA methylation is required for silencing of ant4, an adenine nucleotide translocase selectively expressed in mouse embryonic stem cells and germ cells, Stem Cells 23 (2005) 1314–1323.
[33] S. Giraud, C. Bonod-Bidaud, M. Wesolowski-Louvel, G. Stepien, Expression of human ANT2 gene in highly proliferative cells: GRBOX, a new transcriptional element, is involved in the regulation of glycolytic ATP import into mitochondria, J. Mol. Biol. 281 (1998) 409–418.
[34] C. Bonod-Bidaud, A. Chevrollier, I. Bourasseau, A. Lachaux, B. Mousson de Camaret, G. Stepien, Induction of ANT2 gene expression in liver of patients with mitochondrial DNA depletion, Mitochondrion 1 (2001) 217–224.
[35] A. Chevrollier, D. Loiseau, F. Gautier, Y. Malthiery, G. Stepien, ANT2 expression under hypoxic conditions produces opposite cell-cycle behavior in 143B and HepG2 cancer cells, Mol. Carcinog. 42 (2005) 1–8.
[36] A. Chevrollier, D. Loiseau, B. Chabi, G. Renier, O. Douay, Y. Malthiery, G. Stepien, ANT2 isoform required for cancer cell glycolysis, J. Bioenerg. Biomembr. 37 (2005) 307–316.
[37] A. Chevrollier, D. Loiseau, P. Reynier, G. Stepien, Adenine nucleotide translocase 2 is a key mitochondrial protein in cancer metabolism, Biochim. Biophys. Acta 1807 (2011) 562–567.
[38] J.E. Kokoszka, K.G. Waymire, S.E. Levy, J.E. Sligh, J. Cai, D.P. Jones, G.R. MacGregor, D.C. Wallace, The ADP/ATP translocator is not essential for the mitochondrial permeability transition pore, Nature 427 (2004) 461–465.
[39] V. Giorgio, S. von Stockum, M. Antoniel, A. Fabbro, F. Fogolari, M. Forte, G.D. Glick, V. Petronilli, M. Zoratti, I. Szabo, G. Lippe, P. Bernardi, Dimers of mitochondrial ATP synthase form the permeability transition pore, Proc. Natl. Acad. Sci. U. S. A. 110 (2013) 5887–5892.
[40] P. Bernardi, A. Rasola, M. Forte, G. Lippe, The mitochondrial permeability transition pore: channel formation by F-ATP synthase, integration in signal transduction, and role in pathophysiology, Physiol. Rev. 95 (2015) 1111–1155.
[41] K.N. Alavian, G. Beutner, E. Lazrove, S. Sacchetti, H.A. Park, P. Licznerski, H. Li, P. Nabili, K. Hockensmith, M. Graham, G.A. Porter Jr., E.A. Jonas, An uncoupling channel within the c-subunit ring of the F1FO ATP synthase is the mitochondrial permeability transition pore, Proc. Natl. Acad. Sci. U. S. A. 111 (2014) 10580–10585.
[42] E.A. Jonas, G.A. Porter Jr., G. Beutner, N. Mnatsakanyan, K.N. Alavian, Cell death disguised: the mitochondrial permeability transition pore as the c-subunit of the F(1)F(O) ATP synthase, Pharmacol. Res. 99 (2015) 382–392.
[43] F.K. Teixeira, C.G. Sanchez, T.R. Hurd, J.R. Seifert, B. Czech, J.B. Preall, G.J. Hannon, R. Lehmann, ATP synthase promotes germ cell differentiation independent of oxidative phosphorylation, Nat. Cell Biol. 17 (2015) 689–696.
[44] M.K. Bauer, A. Schubert, O. Rocks, S. Grimm, Adenine nucleotide translocase-1, a component of the permeability transition pore, can dominantly induce apoptosis, J. Cell Biol. 147 (1999) 1493–1502.
[45] M. Zamora, M. Granell, T. Mampel, O. Vinas, Adenine nucleotide translocase 3 (ANT3) overexpression induces apoptosis in cultured cells, FEBS Lett. 563 (2004) 155–160.
[46] M. Zamora, C. Merono, O. Vinas, T. Mampel, Recruitment of NF-kappaB into mitochondria is involved in adenine nucleotide translocase 1 (ANT1)-induced apoptosis, J. Biol. Chem. 279 (2004) 38415–38423.
[47] J.Y. Jang, Y. Choi, Y.K. Jeon, K.C. Aung, C.W. Kim, Over-expression of adenine nucleotide translocase 1 (ANT1) induces apoptosis and tumor regression in vivo, BMC Cancer 8 (2008) 160.
[48] N. Narula, M.V. Zaragoza, P.P. Sengupta, P. Li, N. Haider, J. Verjans, K. Waymire, M. Vannan, D.C. Wallace, Adenine nucleotide translocase 1 deficiency results in dilated cardiomyopathy with defects in myocardial mechanics, histopathological alterations, and activation of apoptosis, JACC Cardiovasc. Imaging 4 (2011) 1–10.
[49] L. Palmieri, S. Alberio, I. Pisano, T. Lodi, M. Meznaric-Petrusa, J. Zidar, A. Santoro, P. Scarcia, F. Fontanesi, E. Lamantea, I. Ferrero, M. Zeviani, Complete loss-of-function of the heart/muscle-specific adenine nucleotide translocator is associated with mitochondrial myopathy and cardiomyopathy, Hum. Mol. Genet. 14 (2005) 3079–3088.
[50] A. Echaniz-Laguna, M. Chassagne, J. Ceresuela, I. Rouvet, S. Padet, C. Acquaviva, S. Nataf, S. Vinzio, D. Bozon, B. Mousson de Camaret, Complete loss of expression of the ANT1 gene causing cardiomyopathy and myopathy, J. Med. Genet. 49 (2012) 146–150.
[51] K.A. Strauss, L. Dubiner, M. Simon, M. Zaragoza, P.P. Sengupta, P. Li, N. Narula, S. Dreike, J. Platt, V. Procaccio, X.R. Ortiz-Gonzalez, E.G. Puffenberger, R.I. Kelley, D.H. Morton, J. Narula, D.C. Wallace, Severity of cardiomyopathy associated with adenine nucleotide translocator-1 deficiency correlates with mtDNA haplogroup, Proc. Natl. Acad. Sci. U. S. A. 110 (2013) 3253–3458.
[52] L.A. Esposito, S. Melov, A. Panov, B.A. Cottrell, D.C. Wallace, Mitochondrial disease in mouse results in increased oxidative stress, Proc. Natl. Acad. Sci. U. S. A. 96 (1999) 4820–4825.
[53] S. O'Gorman, N.A. Dagenais, M. Qian, Y. Marchuk, Protamine-Cre recombinase transgenes efficiently recombine target sequences in the male germ line of mice, but not in embryonic stem cells, Proc. Natl. Acad. Sci. U. S. A. 94 (1997) 14602–14607.

[54] R.E. Braun, R.R. Behringer, J.J. Peschon, R.L. Brinster, R.D. Palmiter, Genetically haploid spermatids are phenotypically diploid, Nature 337 (1989) 373–376.
[55] A.J. Copp, Death before birth: clues from gene knockouts and mutations, Trends Genet. 11 (1995) 87–93.
[56] J. Rossant, Mouse mutants and cardiac development: new molecular insights into cardiogenesis, Circ. Res. 78 (1996) 349–353.
[57] J.R. Hom, R.A. Quintanilla, D.L. Hoffman, K.L. de Mesy Bentley, J.D. Molkentin, S.S. Sheu, G.A. Porter Jr., The permeability transition pore controls cardiac mitochondrial maturation and myocyte differentiation, Dev. Cell 21 (2011) 469–478.
[58] S.W. Cho, J.S. Park, H.J. Heo, S.W. Park, S. Song, I. Kim, Y.M. Han, J.K. Yamashita, J.B. Youm, J. Han, G.Y. Koh, Dual modulation of the mitochondrial permeability transition pore and redox signaling synergistically promotes cardiomyocyte differentiation from pluripotent stem cells, J. Am. Heart Assoc. 3 (2014) e000693.
[59] A. Torroni, G. Stepien, J.A. Hodge, D.C. Wallace, Neoplastic transformation is associated with coordinate induction of nuclear and cytoplasmic oxidative phosphorylation genes, J. Biol. Chem. 265 (1990) 20589–20593.
[60] J.Y. Jang, Y. Choi, Y.K. Jeon, C.W. Kim, Suppression of adenine nucleotide translocase-2 by vector-based siRNA in human breast cancer cells induces apoptosis and inhibits tumor growth in vitro and in vivo, Breast Cancer Res. 10 (2008) R11.
[61] J.Y. Jang, M.K. Kim, Y.K. Jeon, Y.K. Joung, K.D. Park, C.W. Kim, Adenovirus adenine nucleotide translocator-2 shRNA effectively induces apoptosis and enhances chemosensitivity by the down-regulation of ABCG2 in breast cancer stem-like cells, Exp. Mol. Med. 44 (2012) 251–259.
[62] D.G. Wilkinson, M.A. Nieto, Detection of messenger RNA by in situ hybridization to tissue sections and whole mounts, Methods Enzymol. 225 (1993) 361–373.
[63] J.W. Ellison, X. Li, U. Francke, L.J. Shapiro, Rapid evolution of human pseudoautosomal genes and their mouse homologs, Mamm. Genome 7 (1996) 25–30.